

Chemomechanical control of sliding friction behaviour in non-metals

N. H. MACMILLAN, R. D. HUNTINGTON, A. R. C. WESTWOOD

Martin Marietta Laboratories (formerly RIAS), 1450 South Rolling Road, Baltimore, Maryland, USA

Recent work has shown that surface active environments can be used to significantly and predictably influence the near-surface flow behaviour (i.e. hardness) of such solids as magnesium oxide, calcite, alumina, quartz and soda-lime (s.l.) glass. Specifically, these solids are hardest in environments in which their ζ -potential is approximately zero. The results of the present study demonstrate that such chemomechanical effects can, under certain conditions, also be used to affect and control sliding friction behaviour. In particular, it is shown that for magnesium oxide and s.l. glass in various environments the coefficient of friction μ_f is a minimum when $\zeta \approx 0$. This and other results are described, and some mechanistic and practical implications discussed.

1. Introduction

The environment in which sliding takes place can affect frictional behaviour in several ways. If present in sufficient quantity, it may facilitate motion by separating physically the sliding surfaces (complete or hydrodynamic lubrication). Alternatively, as little as a monolayer of adsorbate may interfere markedly with adhesion at regions in contact (boundary lubrication). Both of these effects may be expected to occur for all classes of solids [1]. For inorganic non-metals in particular, however, there is also a third possibility, namely that surface active species adsorbed from a non-corrosive liquid environment may cause some change in the near-surface flow and flow-dependent fracture properties of the sliding solids, and so affect their frictional behaviour. Such an effect may be termed a chemomechanical effect [2]. It has been shown for MgO that chemomechanical effects may persist to depths as great as 30 μm , and that microhardness is greatest, i.e. near-surface dislocation mobility is least, in those environments for which the ζ -potential of the solid is zero [3]. The same phenomenological correlation between microhardness or pendulum hardness and ζ -potential has been demonstrated also in other crystalline solids, e.g. alumina [4], quartz [5] and calcite [6], and in silicate glasses [7, 8]. For such non-metallic solids, therefore, the coefficient of friction, μ_f , might be expected

to vary with environmental composition more or less inversely as the hardness – provided that hydrodynamic lubrication does not occur, and that the sliding surfaces neither contain asperities much larger than a few microns in height nor interpenetrate to depths much greater than this. The studies reported below confirm this conjecture, and reveal that this third influence of environment on μ_f can be the dominant influence under appropriate experimental conditions. Nevertheless, with the exceptions of the work of Dufrane and Glaeser [9] and of Buckley [10, 11], this influence appears to have been largely overlooked in previous friction studies.

This paper presents the initial results of a systematic investigation of the frictional behaviour of (i) MgO in water, n-hexadecane, dimethyl formamide (DMF), dimethyl sulphoxide (DMSO), DMF-DMSO solutions and buffered aqueous 10^{-2} N NaCl solutions, and of (ii) soda lime (s.l.) glass in water, pure n-alcohols, and hexyl alcohol-octyl alcohol solutions. These particular solids were chosen because their variations in hardness (or near-surface dislocation mobility) and/or ζ -potential with composition of the environments noted had already been established.

2. Previous work

Lord Rayleigh [12] appears to have been the

first to observe that μ_f for s.l. glass sliding on s.l. glass is greater in water than in air. As part of a more comprehensive study, Hardy and co-workers subsequently determined μ_f for glass sliding on glass in the homologous series of primary and secondary alcohols [13, 14]. With the exception of three secondary alcohols, it was found for both series that μ_f decreased as the number of carbon atoms in the molecular chain, N_C , increased. More recently, Zisman [15] has reported the influence of condensed monolayers of fatty acids, amines and alcohols of $N_C > 8$ on μ_f for a stainless steel rider sliding on s.l. glass. In all cases, μ_f decreased essentially linearly with N_C , reaching ~ 0.05 at $N_C = 14$ and remaining constant at this value for substances having $N_C > 14$.

The damage produced on cleaved {100} MgO monocrystal surfaces by diamond or sapphire sliders was first studied by Steijn [16]. Bowden and Brookes [17] and Billingham *et al* [18] have since presented detailed accounts of the mechanisms by which the characteristic chevron damage pattern is formed. Bowden *et al* [17, 19] have also studied the influence of slider geometry and normal load on μ_f for MgO in air using both diamond and MgO sliders. Other work by Bowden and Hanwell [20] showed that μ_f for MgO sliding on MgO increases ten-fold as air pressure is reduced from atmospheric to 10^{-10} Torr, with concomitant removal of adsorbed water, etc.

Of particular relevance to the present investigation, however, are the results of studies by Dufrane and Glaeser [9] and Buckley [10, 11] of the influence on the frictional behaviour of MgO and CaF₂ of certain environments known [21-24] to affect to some measurable degree near-surface dislocation mobility in these solids. Dufrane and Glaeser's studies involved repeatedly rolling a hardened steel ball over cleaved and chemically polished {100} MgO surfaces. They noted extensive spalling and subsurface cleavage along rolling contact tracks after 10^8 traverses under toluene, whereas no such damage was evident under water or DMF. They noted also that the tracks were wider and shallower when developed under toluene (~ 250 and ~ 0.3 μm , respectively) than under DMF (~ 100 and 0.5 μm , respectively). Unfortunately, no measurements of μ_f could be obtained from this study. Buckley conducted sliding experiments on the {111} cleavage face of CaF₂ using a 2 mm diameter sapphire ball, sliding speeds of

0.3 to 30 mm min^{-1} , and water, oleic acid, n-hexadecane and DMSO as test environments [10]. μ_f was found to be markedly sensitive to environmental composition, being ~ 0.1 in water, ~ 0.12 in oleic acid, ~ 0.2 in n-hexadecane and ~ 0.3 in DMSO, for loads ranging from 100 to 600 g. Comparative dislocation mobility data are available only for water and DMSO [23, 24], and reveal that $\Delta L(1000)$ for edge dislocations is not markedly different in these two environments. The low value of μ_f for CaF₂ in water as compared to DMSO is, therefore, attributed to the formation of a surface film of Ca(OH)₂, which has a layered structure and hence good "lubricating" properties [10], rather than to any chemomechanical phenomenon.

Most recently, Powers *et al* [25] have noted variations in the damage produced on the {0001} surfaces of fluorapatite (Ca₅F(PO₄)₃) monocrystals in air, water and DMF environments by a diamond slider, with water producing the most severe damage. However, no concomitant differences in μ_f were detected.

3. Experimental

3.1. Test procedures

The apparatus used to determine μ_f is based on a design by Buckley [10], and employs an electric motor to tow a normally loaded slider at a constant speed (0.5 mm min^{-1} throughout the present work) over the surface of a specimen held horizontally and immersed in the chosen test environment. A phosphor bronze proof ring, instrumented with strain gauges, links the slider to the towing arm. The signal from these gauges is fed to a strip chart to provide a continuous record of the towing force required to move the slider. μ_f is defined as the average value of this towing force divided by the normal load applied to the slider.

All measurements made on glass surfaces employed a 6 mm diameter sapphire ball as slider and a normal load of 300 g. The ball used was mechanically ground to a high degree of sphericity, and was covered with fine scratches ~ 1 μm deep. Over a large number of runs these scratches were gradually worn away. However, no measurable change in μ_f was detected due to this slow wear process. Likewise, random changes of the crystallographic orientation of the ball with respect to sliding direction produced no discernible effect on μ_f .

Most of the measurements of μ_f for MgO were

made using a standard 136° Vickers diamond pyramid indenter as slider, and a normal load of 20 g. This slider was usually towed in the "edge-on" orientation, i.e. with two pyramid faces symmetrically inclined about the towing direction. However, in a few cases it was towed in the "side-on", maximum ploughing, orientation, i.e. rotated 45° from the "edge-on" position so that two pyramid edges were equally inclined to the towing direction. A few measurements of μ_f for MgO in water and n-hexadecane employed the sapphire ball slider and a 300 g normal load. Both sliders were thoroughly rinsed and dried between all changes of test environment.

The data points shown in the figures are averages derived from four to twelve experiments in each environment.

3.2. Materials

MgO specimens, approx. $15\text{ mm} \times 5\text{ mm} \times 5\text{ mm}$ in size, were cleaved under the appropriate test environment from large colourless monocrystals of $\sim 99.9\%$ purity*, and kept totally immersed until the measurement of μ_f was completed. In this way, spurious adsorption on the test surface was minimized. All friction traverses were made parallel to $\langle 100 \rangle$. After passage of the slider, the specimens were rinsed in ethyl alcohol, dried, and the resultant tracks examined optically. Subsequently, specimens were re-examined following etching for 3 min at room temperature in a mixture of 5 parts saturated aqueous NH_4Cl :1 part concentrated (98%) H_2SO_4 :1 part H_2O [26] to reveal the extent of dislocation motion along the friction track. In some instances MgO specimens were also cleaved perpendicular to the track and re-etched so that the extent of dislocation motion into the crystal could be assessed. The dislocation etching procedure served also to delineate any surface cracks present.

S.l. glass specimens were prepared by fracturing $75\text{ mm} \times 25\text{ mm} \times \sim 1\text{ mm}$ microscope slides under the appropriate environments using the Outwater-Gerry [27] test geometry (for description, see [28]). These specimens also were kept totally immersed throughout the determination of μ_f . By precise alignment of the specimen in the fracturing jig, it proved possible to run a straight crack down the centre of the slide without using any guiding groove or scribe mark, and so to produce extremely flat fracture surfaces well suited to the present studies. The

*Obtained from the Norton Company, Niagara Falls, Ontario.

friction tracks on the glass surfaces were examined by optical and scanning electron microscopy.

4. Results

4.1. MgO

Fig. 1a presents the variation in μ_f for a Vickers diamond pyramid indenter sliding edge-on on MgO in binary DMSO-DMF solutions. For comparison, the influence of these same environments on near-surface edge dislocation mobility is shown in Fig. 1b [22, 24]. In this figure, the parameter $\Delta L(1000)$ is defined as the increase in the extent of edge-dislocation motion occurring around a diamond pyramid indenta-

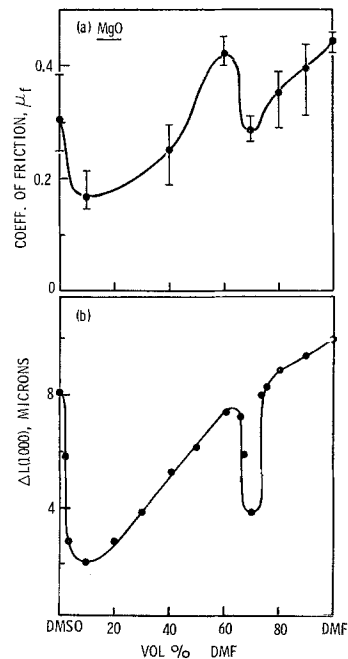


Figure 1 Variation in (a) coefficient of friction (pyramidal indenter, edge-on) and (b) edge dislocation mobility [22, 24] for MgO in DMSO-DMF solutions.

tion made with a 10 g load in a $\{100\}$ cleavage surface when the loading time is increased from 2 to 1000 sec. A similar definition of $\Delta L(1000)$ for screw dislocations is used elsewhere in this paper. Note that $\Delta L(1000)$ is inversely related to microhardness [3, 21, 22], and that the same rather complex variation with environmental composition occurs both for μ_f and $\Delta L(1000)$.

Fig. 2a illustrates the variation of μ_f with pH for the same slider traversing an MgO surface

immersed in aqueous 10^{-2} N NaCl solutions buffered by appropriate additions of NaOH or HCl. Fig. 2b [3] shows the variation of $\Delta L(1000)$ for both near-surface edge and screw dislocations in MgO in the same environments. Again, it is clear that μ_f varies in the same manner as near-surface dislocation mobility – i.e. in the opposite manner to hardness – as environmental composition changes.

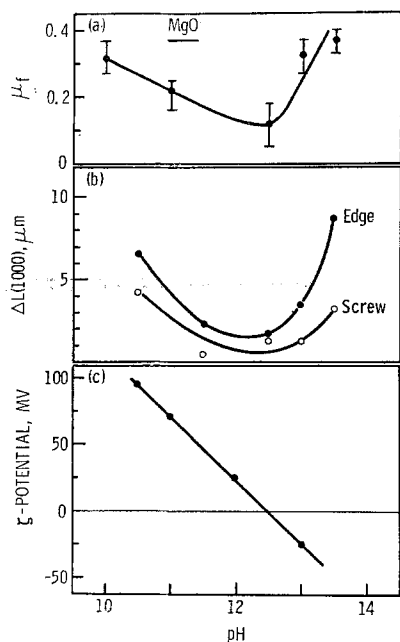


Figure 2 Variation in (a) coefficient of friction (pyramidal indenter, edge-on), (b) near-surface edge and screw dislocation mobilities [3], and (c) ζ -potential [29] for MgO in buffered 10^{-2} N NaCl solutions. Note both $\Delta L(1000)$ and μ_f are least when $\zeta \approx 0$.

Fig. 2c presents the ζ -potential of MgO in these same environments, as determined from streaming potential measurements [29]. From a comparison of Fig. 2a, b and c, it can be seen that both μ_f and edge and screw dislocation mobilities are least when $\zeta \approx 0$. Furthermore, as ζ increases, hardness decreases, and both μ_f and edge and screw dislocation mobilities increase.

μ_f was also determined for MgO in distilled water and n-hexadecane ($\text{C}_{16}\text{H}_{34}$) environments, using both the sapphire ball and Vickers diamond pyramid sliders. Table I summarizes the results and reveals that, for all slider geometries, μ_f is significantly greater in n-hexadecane than in water. Intuitively, this result would not be

TABLE I Coefficient of friction of MgO

Slider	Environment	
	Water	n-hexadecane
Sapphire ball	0.14	0.31
Diamond pyramid (edge-on)	0.19	0.41
Diamond pyramid (side-on)	0.12	0.65

anticipated, since n-hexadecane is an oily, viscous fluid that might be expected to produce a lower value of μ_f than water. However, previous work [24] has established that for edge dislocations in MgO $\Delta L(1000)$ is ~ 12 μm in an n-hexadecane environment but only ~ 2 μm in water. Thus, friction behaviour and environment-sensitive near-surface dislocation behaviour are again simply related. Note that μ_f in hexadecane is greatest when the Vickers diamond pyramid is slid "side-on" – in the maximum ploughing mode – and least when a sapphire ball is used.

Optical microscopy reveals that the relationship between the value of μ_f and the density of cracking along a track, or the distribution of dislocations around or beneath it, is not always simple. Of course, in certain instances greater values of μ_f were accompanied by evidently more severe local deformation. Fig. 3, for example, reveals the greater damage produced when sliding the diamond pyramid over MgO in n-hexadecane ($\mu_f \sim 0.41$) as opposed to water ($\mu_f \sim 0.19$). The increased ploughing associated with the greater value of μ_f in n-hexadecane causes a greater accumulation of plastic flow and results in extensive $\{110\}$ cracking at the surface (Fig. 3b). In contrast, almost no such cracking is seen along the corresponding track formed in water (Fig. 3a). Comparison of Fig. 3c and d reveals also that dislocations penetrate further into the crystal beneath the track when sliding in n-hexadecane than when sliding in water. A less simple feature of the results for the diamond pyramid slider, however, is that the extensive $\{110\}$ cracking shown in Fig. 3b is not reproduced in either DMF ($\mu_f \sim 0.42$) or aqueous 10^{-2} N NaCl buffered to a pH of 13.5 ($\mu_f \sim 0.38$), even though the values of μ_f are similar. In the case of a sapphire ball sliding on MgO in n-hexadecane and water environments ($\mu_f \sim 0.31$ and 0.14, respectively), the damage also is not simply related to μ_f . Thus, although Fig. 4d reveals that greater damage is produced beneath the track in

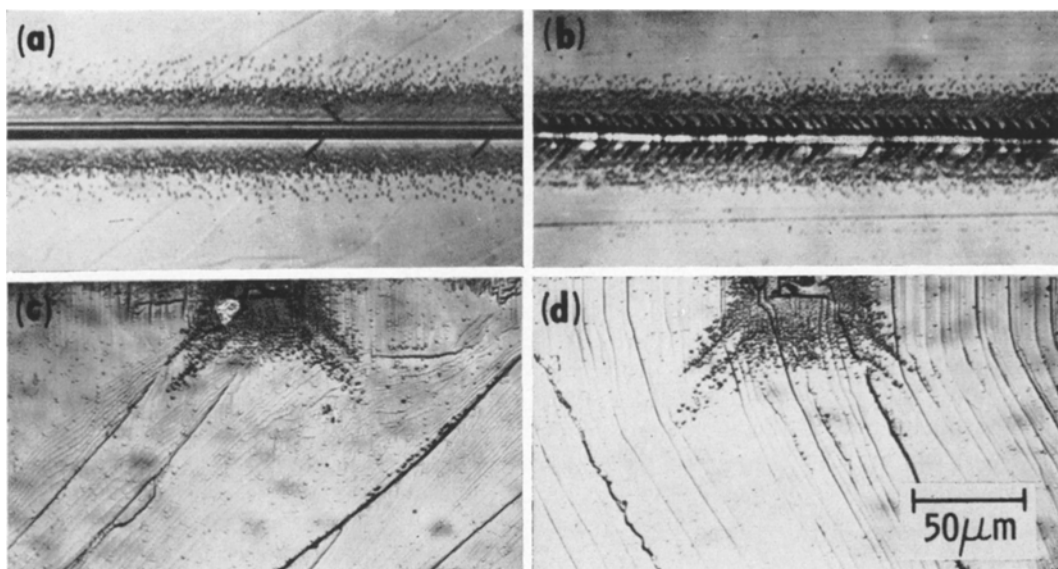


Figure 3 Illustrating effects of water (a and c) and n-hexadecane (b and d) on dislocation distribution around tracks produced by sliding a 136° diamond pyramid indenter edge-on in a $\langle 100 \rangle$ direction on a cleaved $\{100\}$ MgO surface. Note that prolific $\{110\}$ surface cracking produced by sliding under n-hexadecane (b) is not produced under water (a), and that more subsurface damage is produced under n-hexadecane (d) than under water (c).

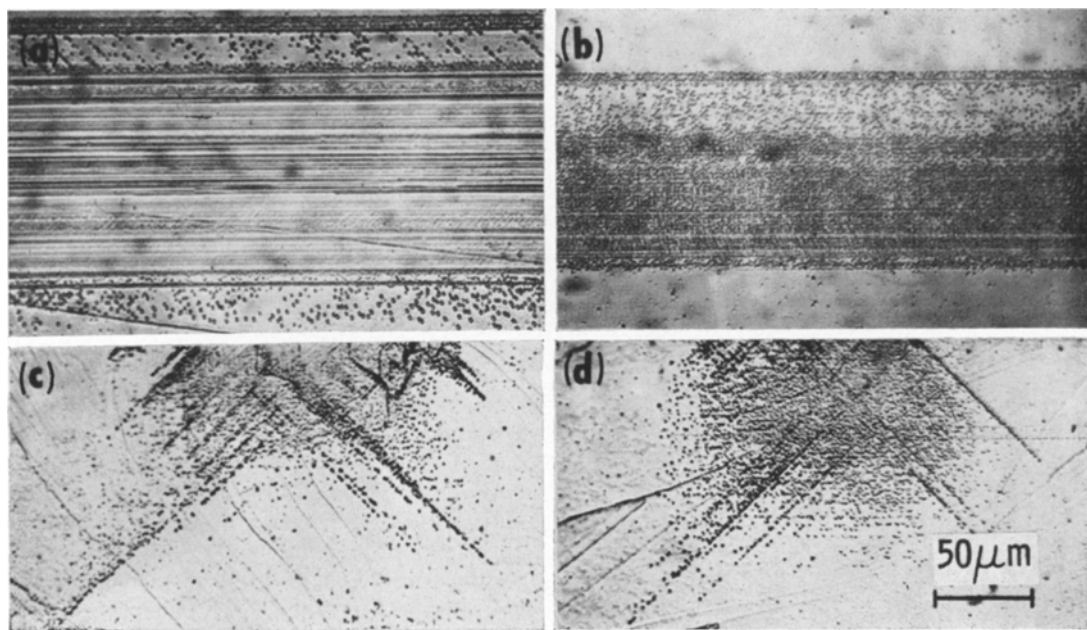


Figure 4 As Fig. 3, but using a 6 mm sapphire ball (300 g load) as slider. The track produced under n-hexadecane which softens MgO – is slightly narrower (b), but subsurface damage is more extensive (d).

n-hexadecane than in water, Fig. 4c, this extra damage is not obvious when the tracks themselves are examined, cf. Fig. 4a and b. Indeed, the track produced under n-hexadecane is slightly narrower than that produced under water.

4.2. S.l. glass

Fig. 5a shows the variation of μ_f with N_C , the number of carbon atoms per molecule of the n-alcohol environment, for the sapphire ball sliding on s.l. glass under a 300 g load. For purposes of comparison, data from Hardy and Doubleday [13] for s.l. glass sliding on itself in the same environments are also included. Fig. 5b illustrates the variation in pendulum hardness of s.l. glass in the same n-alcohols and in water [8], and Fig. 5c the corresponding ζ -potential data

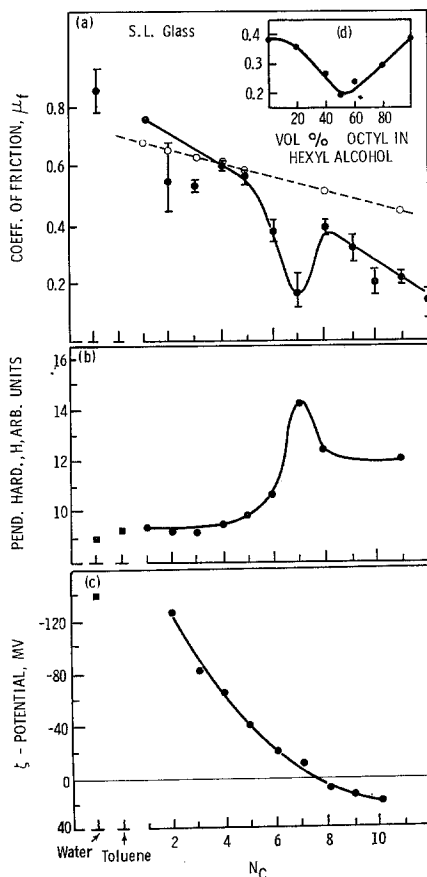


Figure 5 Variation in (a) coefficient of friction, (b) pendulum hardness [8], and (c) ζ -potential [2] of s.l. glass in water and n-alcohol environments. Friction measurements (solid points) employed spherical sapphire slider. Note that μ_f is a minimum and hardness a maximum when $\zeta \simeq 0$. Open circles are earlier data from Hardy and Doubleday [13] for s.l. glass sliding on itself.

for this glass [2]. Despite the considerable scatter found in water and ethyl alcohol environments, the present friction data, like the earlier data of Hardy and Doubleday [13], reveal an essentially linear decrease in μ_f with increasing N_C . However, the slope of the line is different in the two cases. The present data also reveal that, superimposed on this otherwise steady decrease, there is a sharp local minimum in μ_f in heptyl alcohol. This minimum was not reported earlier because Hardy and Doubleday did not use either hexyl or heptyl alcohol environments in their studies. Fig. 5b and c, respectively, show that soda lime glass also exhibits a maximum in hardness and a zero ζ -potential in heptyl alcohol. Hence, a correlation between hardness, μ_f and ζ -potential, phenomenologically similar to that observed in MgO, occurs also for s.l. glass. Essentially, for the experimental conditions employed in this work, hardness is a maximum and μ_f a minimum when $\zeta \simeq 0$.

Fig. 5d demonstrates that the minimum in μ_f observed in heptyl alcohol can be reproduced in the appropriate binary solution of hexyl in octyl alcohol. Other experiments showed that the value of μ_f obtained in water (0.85 ± 0.1) was independent of the load applied to the slider for loads of 25 to 500 g.

SEM studies reveal that the friction tracks formed by the sapphire ball on s.l. glass fracture surfaces immersed in water consist of shallow "plastic" grooves, irregularly pock-marked by "craters" where material apparently has been torn out of the surface, and crossed at right angles to their lengths by series of arc-shaped Hertzian cracks (Fig. 6a). Some of these cracks run the full width of the groove, others only part way across. From their curvature, it is clear that these Hertzian cracks are formed behind the slider, where the elastic tensile stresses are greatest [18, 30]. Craters appear to be formed initially within the arcs of the Hertzian cracks and to extend along the groove in the tracking direction. The frequency and extent of occurrence of the cracks, and more particularly of the craters, may vary considerably along a particular friction track, or between two friction tracks formed under apparently identical conditions. These variations are accurately reflected in the variations of the towing force with distance as recorded on the strip chart. Thus, since μ_f is directly proportional to the average value of this towing force, it is necessary to tow the slider for considerable distances (typically several cm) to obtain a

reliable value of μ_f and to minimize scatter. Regardless of such “random” variations, however, friction track geometry varies significantly with environment. Fig. 6a shows that, with a 300 g load on the sapphire slider, the track produced on s.l. glass in water is a ragged plastic groove, $\sim 100 \mu\text{m}$ wide, whereas that produced in heptyl alcohol (Fig. 6b) shows significant plastic deformation only along a band 20 to 30 μm wide. The latter track also exhibits considerably more frequent, but less extensive, cracking and cratering than the former.

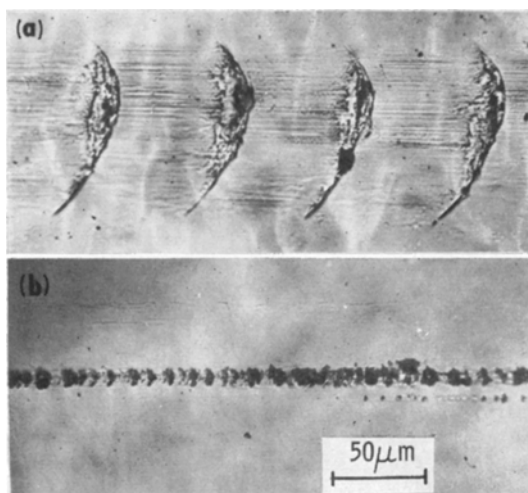


Figure 6 Tracks produced by sapphire ball sliding on s.l. glass under (a) water – note wide track and extensive cracking and cratering associated with μ_f of 0.85, and (b) heptyl alcohol – note narrower track with less surface damage associated with a μ_f of 0.15. Heptyl alcohol maximizes the hardness of s.l. glass, see Fig. 5b.

5. Discussion

This work has established that, when sliding under conditions involving some appreciable degree of ploughing, surface active liquid environments can markedly affect and even control the frictional behaviour of MgO and s.l. glass by influencing their near-surface flow properties (i.e. their microhardness). Moreover, for these solids, since environment-sensitive microhardness is related to ζ -potential [3, 7] (Figs. 2 and 5), μ_f also is dependent to some degree upon this parameter. Specifically, μ_f is a minimum when $\zeta \simeq 0$. And, because the correlation between ζ -potential and hardness (or dislocation mobility) illustrated in Figs. 2 and 5 appears generic to inorganic non-metallic solids, whether

crystalline or non-crystalline [3], a similar dependence of μ_f on ζ -potential may be anticipated under equivalent testing conditions for other inorganic non-metals also.

According to Bowden *et al* [1, 19], the frictional force, F , between sliding solids may be regarded as made up of two parts, the force required to shear adhering junctions in the region of surface contact, and the force to deform the underlying solid. Hence, $F = AS + P$, where A is the real area of contact, S is the shear strength of the contact regions, and P is a deformation (ploughing) term. In experiments such as those undertaken in this work, where significant plastic deformation of the underlying solid does occur during sliding – as evidenced by the well-defined friction tracks left by the slider – F , which is directly proportional to μ_f , is strongly dependent on the magnitude of P . In the present experiments with MgO, therefore, it is probable that environments which affected μ_f did so because of their influence on P . Thus, just as Bowden *et al* [19] were able to influence μ_f for MgO by sliding in different crystallographic directions across a cleaved surface (because MgO is “softer” in a $\{100\}$ direction than in a $\{110\}$ direction), so in this work μ_f in one crystallographic direction has been varied by a factor of three by environmentally influencing the ease of near-surface plastic deformation.

The data of Table I illustrate the role of slider geometry in determining the importance of the environment-sensitive plastic deformation term (P) relative to the adhesion term (AS) in the frictional behaviour of MgO. Compared to water, n-hexadecane is a much more efficient boundary lubricant for a variety of surfaces [13]. Nevertheless, μ_f is greater in n-hexadecane than in water for all slider geometries. Thus, since it is known that n-hexadecane markedly facilitates near-surface dislocation mobility in MgO as compared to water [24], it is clear that environment-sensitive dislocation behaviour, rather than boundary lubrication, determines the magnitude of μ_f in these experiments. Moreover, the difference between μ_f for MgO in water and n-hexadecane increases as the geometry of the indenter is changed to increase the amount of ploughing involved in sliding – i.e. from sapphire ball to pyramid edge-on to pyramid side-on.

When sliding the sapphire ball on s.l. glass, however, Fig. 5a, boundary lubrication appears to play a relatively more important role. In this case, the steady decrease in μ_f with increasing N_C

reflects the greater efficiency of the longer chain n-alcohol molecules as boundary lubricants. Nevertheless, the sharp local minimum superimposed on this steady decrease by heptyl alcohol reveals the influence of environment-sensitive flow. Since viscosity increases with N_C , the fact that μ_t decreases rather than increases with increasing N_C indicates that hydrodynamic lubrication plays no significant role in determining μ_t in these experiments. Of course, this is hardly surprising in view of the slow towing speeds and low viscosities involved.

It is interesting also to note that the minimum at $N_C = 7$ in Fig. 5a can be reproduced in an appropriate binary solution of hexyl in octyl alcohol (Fig. 5d). Previous work [8] has shown that the corresponding hardness maximum, Fig. 5b, can be similarly reproduced in a solution of pentyl in octyl alcohol. This is a significant result because (i) it establishes that the extremum value is real, and not the result of experimental scatter, and (ii) it shows that the extremum is not a consequence of the presence of impurities in the heptyl alcohol used. The behaviour of the binary alcohol solutions is, however, readily explained in terms of the data in Fig. 5c. Hexyl alcohol imparts a negative ζ -potential to s.l. glass while octyl alcohol imparts a positive one. Clearly, therefore, some mixture of the two alcohols will produce $\zeta \simeq 0$, and thereby maximize hardness and minimize μ_t .

This result also implies that, provided boundary lubrication effects are minimized, essentially the same minimum in μ_t can be obtained in *any* environment which produces $\zeta \simeq 0$. Thus, if for some practical application it was desirable to design a liquid environment to minimize μ_t (e.g. to reduce wear in ceramic bearings, or to facilitate the sliding of some specific geological fault in order to minimize stress build-up and the associated earthquake hazard [6, 31]), then an ample choice of ingredients should be available to ensure that the formulation can be appropriately cost-effective, non-toxic and non-polluting.

A detailed understanding of the origin of the " ζ -correlation" (maximum in hardness at $\zeta = 0$), and of the mechanisms by which surface active environments markedly influence surficial flow behaviour, is not yet available. However, for reasons expressed elsewhere [2, 3, 21], such effects are not thought to arise as a consequence of adsorption-induced variations in the surface free energy of the solid. Rather, it is currently

thought [3] that chemomechanical effects occur because charge transfer between adsorbate and solid during chemisorption alters both the surface potential (and therefore the ζ -potential) and also the concentration and distribution of mobile charge carriers in the near-surface region. These changes, it is suggested, affect the ease with which kinks are generated on, and move along, near-surface dislocations in crystals or "dislocation-like" defects [32, 33] in glasses, and hence affect line-defect mobility. For ionic solids, changes in the electron occupancy of near-surface point defects will also influence their interactions with dislocations, and this too will affect dislocation mobility and crystal hardness. The specific role of stress- and surface charge-induced redistributions of mobile non-network ions in determining the near-surface flow behaviour of soda lime glass [7, 8] remains to be defined.

Several aspects of the relationship between the value of μ_t and the size and nature of the corresponding friction track also remain to be explained. For example, μ_t for the diamond pyramid sliding on MgO is essentially the same in n-hexadecane, DMF and aqueous 10^{-2} N NaCl buffered to a pH of 13.5, but considerably more surface cracking occurs under the first of these environments. Perhaps this observation may be rationalized if n-hexadecane produces simultaneously a decrease in adhesion (i.e. in AS) and a relatively larger increase in ploughing (i.e. in P), whereas the other environments merely produce a relatively smaller increase in P . Consistent with this suggestion are the known superior boundary lubrication properties of n-hexadecane [13], and the fact that n-hexadecane measurably enhances edge dislocation mobility in MgO relative to DMF and aqueous 10^{-2} N NaCl at a pH of 13.5 ($\Delta L(1000) \sim 12 \mu\text{m}$ in n-hexadecane [24], cf. $\sim 9 \mu\text{m}$ in the other two environments, Figs. 1b and 2b).

Understanding the relationships between μ_t and extent of surficial damage is even less clear for observations made using the sapphire ball slider. This may be due in part to the near parallelism of slider and substrate surfaces in the "contact area", which makes this "area" very sensitive to any vertical displacement of the slider due to deformation processes occurring beneath it, and in part to the change in "contact angle" between slider and substrate as the former penetrates the latter. For a spherical indenter, however, whether it rolls or slides, any increase

in adhesion both increases the maximum Hertzian (elastic) shear stress occurring beneath the slider and causes this maximum to occur nearer the surface [30]. Thus, increased adhesion might be expected to result in increased sub-surface dislocation nucleation over a wider but shallower area. The effect of such a change on the width of the friction track, as revealed by dislocation etch-pitting methods, will depend on slip geometry, on the relative changes in width and depth of the region where dislocations are nucleated, and on whether such subsurface dislocations as are nucleated, and do reach the surface, do so inside or outside the "contact area". At the same time, any chemomechanically induced increase in near-surface dislocation mobility will allow the solid to better conform plastically to the slider. This also should produce increased subsurface deformation, a wider plastic groove, and less tendency for elastic relaxation after passage of the slider.

In this view, therefore, the most consistent feature of an increase in μ_f , whether due to an increase in ploughing or adhesion or both, should be an increase in sub-surface deformation. Comparison of Fig. 4c and d shows this to be the case for the sapphire ball sliding on MgO when the environment is changed from water to n-hexadecane. The concomitant slight reduction in track width at the higher μ_f value, cf. Fig. 4a and b, remains unexplained. It is interesting to note, however, that Dufrane and Glaeser [9] obtained a narrower track when rolling a steel ball on MgO in DMF than when the same experiment was performed in toluene. Although no measurements of μ_f were made in this latter study, it is reasonable to suppose that the narrower track again corresponds to the higher μ_f value, for dislocation mobility in MgO is much greater in DMF than in toluene [21, 22].

Detailed interpretation of the tracks produced on s.l. glass by the sapphire ball is complicated by lack of knowledge of the mechanisms of flow in this material. It is clear, however, that more extensive plastic flow occurs under a water environment ($\mu_f \sim 0.85$) Fig. 6a, than under heptyl alcohol ($\mu_f \sim 0.15$), Fig. 6b. In the former case, a wide, ragged plastic groove remains, approximately equal in width to the diameter of the circle of contact as calculated from the Hertzian theory of elastic contact ($\sim 95 \mu\text{m}$), showing that plastic flow occurred over the whole "area of contact". In contrast, significant permanent deformation is optically visible only

over the centre 20 to 30 μm of this area in the latter case, demonstrating the hardening influence and superior boundary lubrication properties of heptyl alcohol as compared to water.

Finally, it is of interest to compare the present values of μ_f with those obtained by earlier workers. In the case of s.l. glass, the present data reflect Rayleigh's observation [12] that μ_f is large in water, and are consistent with the observations of Hardy *et al* [13, 14] (see also Fig. 6a) and of Zisman [15] that μ_f for this material decreases with increasing N_C in n-alcohol environments. The different slopes in the plots of μ_f versus N_C obtained by Hardy and Doubleday [13] and by the present authors, Fig. 6a, are presumed to result from the different choice of slider material in the two cases.

Acknowledgements

It is a pleasure to acknowledge helpful discussions with Dr W. M. Mularie, and the experimental assistance of D. H. Taylor and G. H. Parr during the course of this work, which was supported in part by the US Geological Survey under Contract No. 14-08-0001-13077, ARPA Order 1684, and the US Office of Naval Research under Contract No. N00014-70-C-0330.

References

1. F. P. BOWDEN and D. TABOR, "The Friction and Lubrication of Solids", Vol. I (revised) and Vol. II (O.U.P., 1954, 1964).
2. A. R. C. WESTWOOD and N. H. MACMILLAN, "Science of Hardness Testing" (ASM, Cleveland, Ohio 1973) p. 377.
3. N. H. MACMILLAN, R. D. HUNTINGTON and A. R. C. WESTWOOD, *Phil. Mag.* **28** (1973) 923.
4. A. R. C. WESTWOOD, N. H. MACMILLAN and R. S. KALYONCU, *J. Amer. Ceram. Soc.* **56** (1973) 258.
5. *Idem*, *Trans. AIME (Mining)*, in press.
6. A. R. C. WESTWOOD and N. H. MACMILLAN, Martin Marietta Labs., Rept. to US Geological Survey on Contract No. 14-08-0001-13077 (January 1973).
7. A. R. C. WESTWOOD and R. D. HUNTINGTON, "Mechanical Behavior of Materials" Vol. IV (*Soc. Materials Sci. Japan*, Kyoto, Japan, 1972) p. 383.
8. A. R. C. WESTWOOD, G. H. PARR and R. M. LATANISON, "Amorphous Materials" (Wiley, London, 1972) p. 533.
9. K. F. DUFRANE and W. A. GLAESER, Battelle Mem. Inst., Columbus, Ohio, Tech. Repts. on NASA Contract No. NAS-3-6263 (September 1967) and (April 1969).
10. D. H. BUCKLEY, NASA Tech. Rept. TN D-5580 (1969).

11. *Idem*, *Ceram. Bull.* **51** (1972) 884.
12. LORD RAYLEIGH, *Phil. Mag.* **35** (1918) 157.
13. W. B. HARDY and I. DOUBLEDAY, *Proc. Roy. Soc. (London)* **A100** (1922) 550.
14. I. DOUBLEDAY, *J. Chem. Soc.* **121** (1922) 2875.
15. W. A. ZISMAN, "Friction and Wear" (Elsevier, Amsterdam, 1959) p. 110.
16. R. P. STEIJN, *J. Appl. Phys.* **34** (1963) 419.
17. F. P. BOWDEN and C. A. BROOKES, *Proc. Roy. Soc. (London)* **A295** (1966) 244.
18. P. R. BILLINGHURST, C. A. BROOKES and D. TABOR, "Physical Basis of Yield and Fracture" (Inst. Phys. Physical Soc., London, 1966) p. 253.
19. F. P. BOWDEN, C. A. BROOKES and A. E. HANWELL, *Nature (London)* **203** (1964) 27.
20. F. P. BOWDEN and A. E. HANWELL, *Proc. Roy. Soc. (London)* **A295** (1966) 233.
21. A. R. C. WESTWOOD, D. L. GOLDHEIM and R. G. LYE, *Phil. Mag.* **16** (1967) 505.
22. *Idem*, *ibid* **17** (1968) 951.
23. *Idem*, *J. Appl. Phys.* **39** (1968) 3401.
24. *Idem*, *J. Amer. Ceram. Soc.* **53** (1970) 142.
25. J. M. POWERS, R. G. CRAIG and K. C. LUDEMA, *Wear* **23** (1973) 209.
26. R. J. STOKES, T. L. JOHNSTON and C. H. LI, *Phil. Mag.* **3** (1958) 718.
27. J. O. OUTWATER and D. J. GERRY, Univ. of Vermont, Vt. Rept. on Contract No. 2-3219(01)(x), (August 1966).
28. A. G. EVANS, *J. Mater. Sci.* **7** (1972) 1137.
29. MC D. ROBINSON, J. A. PASK and D. W. FUERSTENAU, *J. Amer. Ceram. Soc.* **47** (1964) 516.
30. G. M. HAMILTON and L. E. GOODMAN, *J. Appl. Mech.* **33** (1966) 371.
31. A. R. C. WESTWOOD, Martin Marietta Laboratories, TP-386 (July 1971).
32. J. J. GILMAN, *J. Appl. Phys.* **44** (1973) 675.
33. M. F. ASHBY and J. LOGAN, *Scripta Met.* **7** (1973) 513.

Received 30 July and accepted 26 November 1973.